UC Davis
UC Davis Previously Published Works

Title

PCB 136 Atropselectively Alters Morphometric and Functional Parameters of Neuronal Connectivity in Cultured Rat Hippocampal Neurons via Ryanodine Receptor-Dependent Mechanisms

Permalink

https://escholarship.org/uc/item/28r3887t

Journal

Toxicological Sciences, 138(2)

ISSN

1096-6080

Authors

Yang, Dongren
Kania-Korwel, Izabela
Ghogha, Atefeh
et al.

Publication Date

2014-04-01

DOI

10.1093/toxsci/kft334

Peer reviewed

PCB 136 Atropselectively Alters Morphometric and Functional Parameters of Neuronal Connectivity in Cultured Rat Hippocampal Neurons via Ryanodine Receptor-Dependent Mechanisms

Dongren Yang,[*] Izabela Kania-Korwel,[†] Atefeh Ghogha,[*] Hao Chen,[*] Marianna Stamou,[*] Diptiman D. Bose,[*] Isaac N. Pessah,[*] Hans-Joachim Lehmler,[†] and Pamela J. Lein[*,1]

[*]*Department of Molecular Biosciences, School of Veterinary Medicine, University of California, Davis, California 95616; and* [†]*Department of Occupational and Environmental Health, College of Public Health, University of Iowa, Iowa City, Iowa 52242*

[1]To whom correspondence should be addressed at Department of Molecular Biosciences, UC Davis School of Veterinary Medicine, 2009 VM3B, 1089 Veterinary Medicine Drive, Davis, CA 95616. Fax: (530) 752-7690. E-mail: pjlein@ucdavis.edu.

We recently demonstrated that polychlorinated biphenyl (PCB) congeners with multiple *ortho* chlorine substitutions sensitize ryanodine receptors (RyRs), and this activity promotes Ca^{2+}-dependent dendritic growth in cultured neurons. Many *ortho*-substituted congeners display axial chirality, and we previously reported that the chiral congener PCB 136 (2,2′,3,3′,6,6′-hexachlorobiphenyl) atropselectively sensitizes RyRs. Here, we test the hypothesis that PCB 136 atropisomers differentially alter dendritic growth and other parameters of neuronal connectivity influenced by RyR activity. (−)-PCB 136, which potently sensitizes RyRs, enhances dendritic growth in primary cultures of rat hippocampal neurons, whereas (+)-PCB 136, which lacks RyR activity, has no effect on dendritic growth. The dendrite-promoting activity of (−)-PCB 136 is observed at concentrations ranging from 0.1 to 100nM and is blocked by pharmacologic RyR antagonism. Neither atropisomer alters axonal growth or cell viability. Quantification of PCB 136 atropisomers in hippocampal cultures indicates that atropselective effects on dendritic growth are not due to differential partitioning of atropisomers into cultured cells. Imaging of hippocampal neurons loaded with Ca^{2+}-sensitive dye demonstrates that (−)-PCB 136 but not (+)-PCB 136 increases the frequency of spontaneous Ca^{2+} oscillations. Similarly, (−)-PCB 136 but not (+)-PCB 136 increases the activity of hippocampal neurons plated on microelectrode arrays. These data support the hypothesis that atropselective effects on RyR activity translate into atropselective effects of PCB 136 atropisomers on neuronal connectivity, and suggest that the variable atropisomeric enrichment of chiral PCBs observed in the human population may be a significant determinant of individual susceptibility for adverse neurodevelopmental outcomes following PCB exposure.

Key Words: atropselectivity, chirality, dendritic growth, developmental neurotoxicity, neuronal connectivity, polychlorinated biphenyls, ryanodine receptor.

Polychlorinated biphenyls (PCBs) have been identified as probable environmental risk factors for neurodevelopmental disorders (Landrigan *et al.*, 2012; Stamou *et al.*, 2013; Winneke, 2011). This conclusion is based in large part on epidemiological data demonstrating a negative association between developmental exposure to PCBs and measures of neuropsychological function in infancy or childhood (Boucher *et al.*, 2009; Carpenter, 2006; Korrick and Sagiv, 2008; Schantz *et al.*, 2003; Winneke, 2011). But it also derives from studies demonstrating that despite a ban on their production in 1977, PCBs persist at high concentrations in the environment and in animal and human tissues (Lehmler *et al.*, 2010; Marek *et al.*, 2013). Recent reports from the United States confirm widespread exposure to PCBs among women of childbearing age (Thompson and Boekelheide, 2013) and document levels of PCBs in the indoor air of elementary schools that exceed the United State Environmental Protection Agency (USEPA) 2009 public health guidelines (Thomas *et al.*, 2012). Current PCB exposures are likely due to secondary sources of legacy PCBs, e.g., release from building materials such as caulking and paint (Jamshidi *et al.*, 2007; Thomas *et al.*, 2012) or volatilization from large bodies of water such as the Great Lakes (Hornbuckle *et al.*, 2006), as well as contemporary unintentional sources, most notably commercial paint pigments (Hu and Hornbuckle, 2010).

Research efforts have historically focused on the toxicity of dioxin-like PCBs; however, emerging evidence suggests that non-dioxin-like (NDL) PCBs with multiple *ortho* chlorine substitutions are particularly stable and predominate over dioxin-like congeners in environmental samples (Hwang *et al.*, 2006; Kostyniak *et al.*, 2005; Martinez and Hornbuckle, 2011) and in human tissues (DeCaprio *et al.*, 2005; Marek *et al.*, 2013; Megson *et al.*, 2013; Schantz *et al.*, 2010). NDL PCBs have been shown to interfere with normal neurodevelopment *in vivo* (Kenet *et al.*, 2007; Schantz *et al.*, 1997; Winneke, 2011; Yang *et al.*, 2009) and to modulate neuronal connectivity via effects
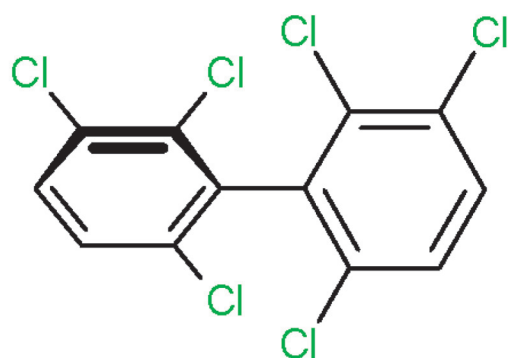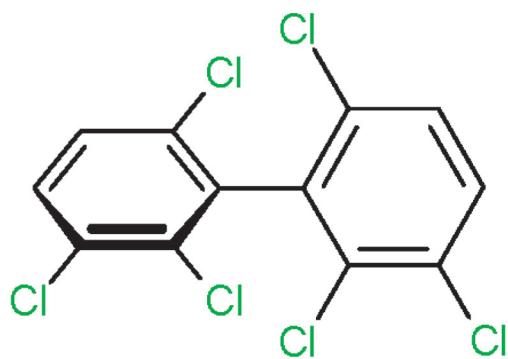
FIG. 1. Structure of PCB 136 atropisomers.

on dendritic arborization both *in vivo* and *in vitro* (Wayman *et al.*, 2012a,b; Yang *et al.*, 2009). The effects of NDL PCBs on dendritic growth are mediated by sensitization of ryanodine receptors (RyRs) (Wayman *et al.*, 2012b), which form Ca^{2+} channels that control Ca^{2+} release from endoplasmic reticulum (ER) stores (Pessah *et al.*, 2010). RyR activity is implicated in the regulation of neurodevelopmental processes that are critical determinants of neuronal connectivity (Pessah *et al.*, 2010), and in primary neuronal cell cultures, RyR sensitization by PCB 95, a NDL PCB congener, triggers a Ca^{2+}-dependent signaling pathway that links activity to dendritic growth (Wayman *et al.*, 2012a).

Many RyR-active PCBs possess an axis of chirality about which the chlorine substituents are held in a spatial arrangement that is not superimposable on its mirror image (Fig. 1); however, under physiological conditions, only 19 of these chiral PCBs, including PCB 136, exist as stable rotational isomers, called atropisomers, and thus can be isolated as purified atropisomers (Lehmler *et al.*, 2010). These chiral PCBs are present in technical mixtures as a racemate (a 1:1 mixture of both atropisomers), but display highly variable atropisomeric enrichment in environmental and human samples, likely as a result of atropselective metabolism by cytochrome P450 enzymes (Warner *et al.*,

2009; Wu *et al.*, 2011). An emerging question is the toxicological relevance of atropisomeric enrichment of chiral PCBs in human populations. Molecular insight regarding this question was provided by our previous study demonstrating that PCB 136, a chiral congener, exhibits atropisomeric specificity toward RyRs (Pessah *et al.*, 2009). Specifically, (−)-PCB 136 potently sensitizes RyRs, whereas (+)-PCB 136 has no effect on RyR activity. The objective of this study was to determine whether the atropselective interactions of PCB 136 with RyRs translate into atropselective effects on morphological and functional parameters of neuronal connectivity.

MATERIALS AND METHODS

Separation of PCB 136 atropisomers. The atropisomers of 2,2′,3,3′,6,6′-hexachlorobiphenyl (PCB 136) were obtained as described previously (Kania-Korwel *et al.*, 2008). The purity of atropisomers was 99% for (−)-PCB 136 and 100% for (+)-PCB 136. The preparation of 4-hydroxy-2,2′,3,3′,6,6′-hexachlorobiphenyl (4-OH PCB 136), 5-hydroxy-2,2′,3,3′,6,6′-hexachlorobiphenyl (5-OH PCB 136), and 4,5-dimethoxy-2,2′,3,3′,6,6′-hexachlorobiphenyl (4,5-OH PCB136) has been published previously (Waller *et al.*, 1999). Analytical PCB standards were obtained from Accustandard (New Haven, CT).

Animals. Animals were treated humanely and with regard to alleviation of suffering according to protocols approved by the Institutional Animal Care and Use Committee of the University of California, Davis. Timed pregnant Sprague Dawley rats were purchased from Charles River Laboratories (Hollister, CA) and housed individually in standard plastic cages with Alpha-Dri bedding (Shepherd Specialty Papers, Watertown, TN) in a temperature ($22 \pm 2°C$) controlled room on a 12 h reverse light-dark cycle. Food and water were provided *ad libitum*.

Tissue culture. Primary cultures of dissociated hippocampal neurons were set up and maintained as previously described (Wayman *et al.*, 2006). Briefly, hippocampi were dissected from postnatal day 1 (P1) rat pups, plated at 7.5×10^4 cells per cm^2 onto glass coverslips or tissue culture plastic precoated with poly-L-lysine (molecular weight 300,000; Sigma, St Louis, MO) and maintained in Neurobasal A media (Invitrogen, Carlsbad, CA) supplemented with B27 (Invitrogen), 2mM glutamax (Invitrogen), and 5μM cytosine-D-arabinofuranoside (Sigma). Half of the medium was replaced with fresh Neurobasal-A containing B27 twice weekly. Unless otherwise noted, PCB exposures were initiated at 7 days *in vitro* (DIV) by diluting DMSO stocks of PCB 136 1:1000 (vol/vol) into culture medium. Vehicle control cultures were exposed to DMSO at 1:1000 (vol/vol).

Quantification of neuronal morphology. For studies of dendritic growth, cultures were transfected at 6 DIV with a pCAGGS expression vector encoding a microtubule-associated

protein-2B (MAP2B)-enhanced green fluorescent protein (eGFP) fusion construct (Wayman *et al.*, 2006) using Lipofectamine 2000 (Invitrogen) according to the manufacturer's protocol. Dr. Gary Wayman (University of Washington, Pullman, WA) generously provided the MAP2B-eGFP fusion construct. Transfection efficiency for MAP2B-eGFP was 0.5–5%. At the end of the PCB exposure, cultures were fixed in fixation buffer (4% paraformaldehyde, 4% sucrose, 60mM Pipes, 25mM Hepes, 5mM EGTA, 1mM $MgCl_2$, pH7.4) for 20 min at room temperature. Coverslips were mounted on glass slides and digital images of GFP-positive neurons at ×200 magnification were analyzed using NeuronJ imaging software (Meijering *et al.*, 2004). Total dendritic length was measured in at least 30 neurons from three coverslips per treatment group, and the experiment was repeated at least three times with cultures prepared from independent dissections.

To quantify the effects of PCB 136 on early stages of axonal growth, hippocampal neurons (3×10^4 cells per cm^2) were treated with (−)-PCB 136 or (+)-PCB 136 starting 3 h after plating, transfected 24 h after plating with a pCAG expression vector encoding tomato fluorescent protein (TFP) (generously provided by Dr. Gary Wayman, University of Washington, Pullman, WA) using Lipofectamine 2000 and then fixed 48 h after plating as described above. Axons were visualized by epifluorescence microscopy at ×200 and axonal lengths quantified using NeuronJ imaging software. Total axonal length was measured in at least 30 neurons from three coverslips per treatment group, and the experiment was repeated twice with cultures prepared from independent dissections.

To analyze axonal growth in mature cultures following exposures identical to those used in the dendritic growth assays, we used Western blotting to quantify the expression of the dephosphorylated form of the cytoskeletal protein tau, an axonal biomarker (Hayashi *et al.*, 2002). Neurons dissociated from P1 rat hippocampi were plated at high density (650 K per well in 6-well plate). At 7 DIV, cultures were treated with vehicle, (−)-PCB 136 or (+)-PCB 136 at concentrations ranging from 0.1nM to 1000nM. After 48 h of exposure, cultures were lysed with ice-cold buffer containing 20mM HEPES (pH 7.4), 150mM NaCl, 1% TritonX-100, 10% glycerol, and 1X complete protease inhibitor cocktail (Roche Applied Science, Indianapolis, IN). The protein concentration of lysates was determined using the BCA Protein Assay (Pierce, Rockford, IL) and 10 μg of each sample was separated using 12% SDS-PAGE then transferred to polyvinylidene fluoride (PVDF) membrane. Membranes were blocked with Odyssey Blocking Buffer (LI-COR, Lincoln, NE) and then incubated overnight at 4°C with mouse monoclonal antibody that recognizes dephosphorylated tau (Millipore, Billerica, MA) and rabbit anti-GAPDH monoclonal antibody (Cell Signaling Technology, Danvers, MA) diluted 1:1000 in Licor blocking buffer. After washing in phosphate buffered saline (PBS) containing 0.1% tween-20, membranes were incubated with goat anti-mouse IgG conjugated to infrared dye (IR)700 (LI-COR) and goat anti-rabbit IgG conjugated to IR800 (LI-

COR) diluted 1:2000 in Odyssey Blocking Buffer for 1.5 h at room temperature. After extensive rinsing, membranes were scanned using the Odyssey Infrared Imaging System (LI-COR). Densitometry values of tau immunopositive bands were normalized to densitometry values for GAPDH-immunopositive bands in the same sample and the data presented as the percentage of the GAPDH-normalized tau densitometry of vehicle controls from the same experiment. This experiment was replicated three times using cell lysates obtained from three independent dissections.

Cytotoxicity assay. Cytotoxicity was assessed using the MTT (3-(4,5-dimethylthiazol-2-yl)-2,5-diphenyltetrazolium bromide) and CytoTox-One lactate dehydrogenase (LDH) release assays available from Promega (Madison, WI) according to the manufacturer's protocol. Each treatment condition was assayed in 12 wells per treatment and experiments were repeated using cultures obtained from three independent dissections.

Analysis of PCB 136 and its hydroxylated metabolites. PCB 136 and its hydroxylated metabolites were extracted from tissue culture plates, cell pellets, and medium using previously published methods (Kania-Korwel *et al.*, 2010). Briefly, all samples were first spiked with surrogate recovery standards (2,3,4,4′,5,6-hexachlorobiphenyl, 500 ng each; cell pellets and medium also with 4-hydroxy-2,3,3′,4,5,5′-hexachlorobiphenyl, 137 ng each). Tissue culture plates were washed repeatedly with hexane-MTBE (1:1, vol/vol; 5 ml). Cell pellet and medium samples were denatured with hydrochloric acid (6M, 1 ml) and extracted with hexane-MTBE (1:1, vol/vol; 4 ml). Hydroxylated PCB 136 metabolites were separated from PCBs by partitioning with potassium hydroxide as described previously (Kania-Korwel *et al.*, 2010) and derivatized with diazomethane. The solvent was exchanged to hexane if appropriate. All samples were spiked with the internal standard (PCB 30 and PCB 204, 200 ng each) and, if necessary, subjected to a sulfuric acid clean-up as published earlier (Kania-Korwel *et al.*, 2010). All extracts were analyzed on an Agilent 6890N gas chromatograph equipped with a micro electron capture detector. Details regarding the capillary columns, temperature programs, and other instrumental parameters used for the conventional and atropselective analysis of PCB 136 and its metabolites are summarized in Supplementary Table S1. The average percent of the surrogate recovery standard recovered from each sample was $107 \pm 6\%$, $91 \pm 18\%$, and $80 \pm 14\%$ for incubation plates, cell pellets, and medium samples, and the PCB 136 solution used in the cell culture experiments, respectively. The detection limit, calculated based on extraction blanks, was 2 ng for PCB 136, 0.21 ng for 4–136, 0.22 ng for 5–136, and 0.04 ng for 4,5–136.

Calcium imaging. To measure Ca^{2+} transients, dissociated hippocampal neurons (7 DIV) were loaded with 5μM Fluo-4 AM (Invitrogen) and imaged as previously described (Wayman

et al., 2012a). Vehicle, (−)-PCB 136, or (+)-PCB 136 dissolved in imaging buffer (140mM NaCl, 5mM KCl, 2mM MgCl$_2$, 2mM CaCl$_2$, 10mM HEPES, and 10mM glucose, pH 7.4 supplemented with 0.05% bovine serum albumin) were perfused on the cells for 10 min. The data were analyzed using origin 8.5 software (OriginLab Corporation, MA). The number of oscillations was counted for each treatment group with oscillations identified as Ca^{2+} transients twice the amplitude of the baseline.

Analysis of activity using microelectrode arrays. Dissociated hippocampal neurons were plated onto microelectrode arrays (MEAs) with a central 0.88 mm^2 recording matrix of 64 multi-electrodes (Med-P545A, AutoMate Scientific, Berkeley, CA) that were precoated with poly-L-lysine (0.5 mg/ml, Sigma) and laminin (10 µg/ml, Invitrogen) at a density of 1 × 10^5 cells/MEA. Cultures were maintained as described above. The development of spontaneous activity in primary neuronal cell cultures plated on MEAs is dependent on neuronal cell type, cell density, and time in culture (Robinette *et al.*, 2011). Pilot studies indicated that under these culture conditions, spontaneous activity as detected using MEA technology increased rapidly between 7–15 DIV and then became relatively stable between DIV 17–24. Thus, for these studies, spontaneous activity was assessed at 21 DIV. At 21 DIV, MEA cultures were placed into the MED 64CH Integrated Amplifier interface and spike activity recorded using Mobius software (AutoMate Scientific). Baseline activity was recorded for 10 min at 37°C. Cultures were then exposed to vehicle by adding 1 µl of DMSO into MEA cultures containing 1 ml of culture medium (final 0.1% DMSO), and activity recorded for 10 min. Cultures were exposed to either (−)-PCB 136 or (+)-PCB 136 by adding culture medium containing the PCB 136 atropisomer to the well. Cultures were sequentially exposed to increasing concentrations of the same PCB atropisomer and activity recorded for 10 min following each addition. Using the Spike Sorting and DC filter applications in Mobius, spikes at least three times baseline were counted and the spontaneous spike activity reported as the number of spikes per 10 min recording session (for electrodes showing activity) and the percent change in the number of active electrodes within the MEA (referred to as percent change in channel activity in figures). Three MEAs from three independent dissections were analyzed per PCB treatment.

Statistical analyses. Data are presented as the mean ± SEM. With the exception of the Ca^{2+} imaging data (number of oscillations per 10 min), which were analyzed by unpaired Student's *t*-test, all data were analyzed by one-way ANOVA ($p < 0.05$) followed by Tukey's *post hoc* test.

RESULTS

Effects of PCB136 Atropisomers on Morphometric Parameters of Neuronal Connectivity

As a first test of the hypothesis that PCB 136 atropselectively influences parameters of neuronal connectivity regulated by RyR activity (Pessah *et al.*, 2010; Wayman *et al.*, 2012b), we compared dendritic growth in primary hippocampal cultures exposed to (−)-PCB 136 versus (+)-PCB 136, which have differential effects on RyR activity (Pessah *et al.*, 2009). To visualize dendritic arbors of individual neurons in high-density neuron-glia co-cultures, cultures were transfected with a MAP2B-eGFP construct under the control of the *CAG* promoter, which exhibits neuron-specific expression (Wayman *et al.*, 2006). Expression of MAP2B-eGFP is restricted to the somatodendritic compartment of cultured hippocampal neurons and does not alter their intrinsic dendritic growth patterns (Wayman *et al.*, 2006). Under the culture conditions used for these experiments, the most rapid expansion of the dendritic arbor occurs between 5–10 DIV (Wayman *et al.*, 2006). Exposure between 7–9 DIV to (−)-PCB 136, which is a potent RyR sensitizer (Pessah *et al.*, 2009), significantly increased total dendritic length in hippocampal neurons (Figs. 2A and B). In contrast, exposure to the same concentration range of (+)-PCB 136, which has negligible activity toward RyRs (Pessah *et al.*, 2009), had no effect on dendritic growth in sister cultures (Fig. 2C). The dendrite-promoting activity of (−)-PCB 136 exhibited a non-monotonic concentration-dependent relationship although the concentrations at which no effects were observed varied between cultures from different dissections. When data from three independent dissections were combined, dendritic growth was observed to be significantly enhanced at concentrations ranging from 0.1 to 100nM but returned to baseline levels at a concentration of 1µM (Fig. 2B). However, analysis of data from each individual dissection indicated that there was no significant increase in dendritic length in neurons exposed to (−)-PCB 136 at 0.1nM in two of three independent dissections; and in one of the three independent dissections, (−)-PCB 136-enhanced dendritic length was not statistically significant at 1nM. We did, however, consistently observe significantly increased dendritic length in neurons exposed to (−)-PCB 136 at 10nM across all three dissections. The dendrite-promoting activity of (−)-PCB 136 was suppressed by the RyR antagonist FLA365 (Chiesi *et al.*, 1988; Mack *et al.*, 1992) (Fig. 2D).

RyRs are expressed in not only dendrites (Seymour-Laurent and Barish, 1995; Wayman *et al.*, 2012a) but also axons (Hertle and Yeckel, 2007), and RyR activity has been implicated in the regulation of axonal growth and guidance (Ooashi *et al.*, 2005; Welshhans and Rehder, 2007). Thus, we next determined whether PCB 136 exerts atropselective effects on axonal growth. It is extremely difficult to delineate the entire axonal plexus extended by a single neuron in mature (> 3 DIV) cultures because axons continue to elongate over time in culture
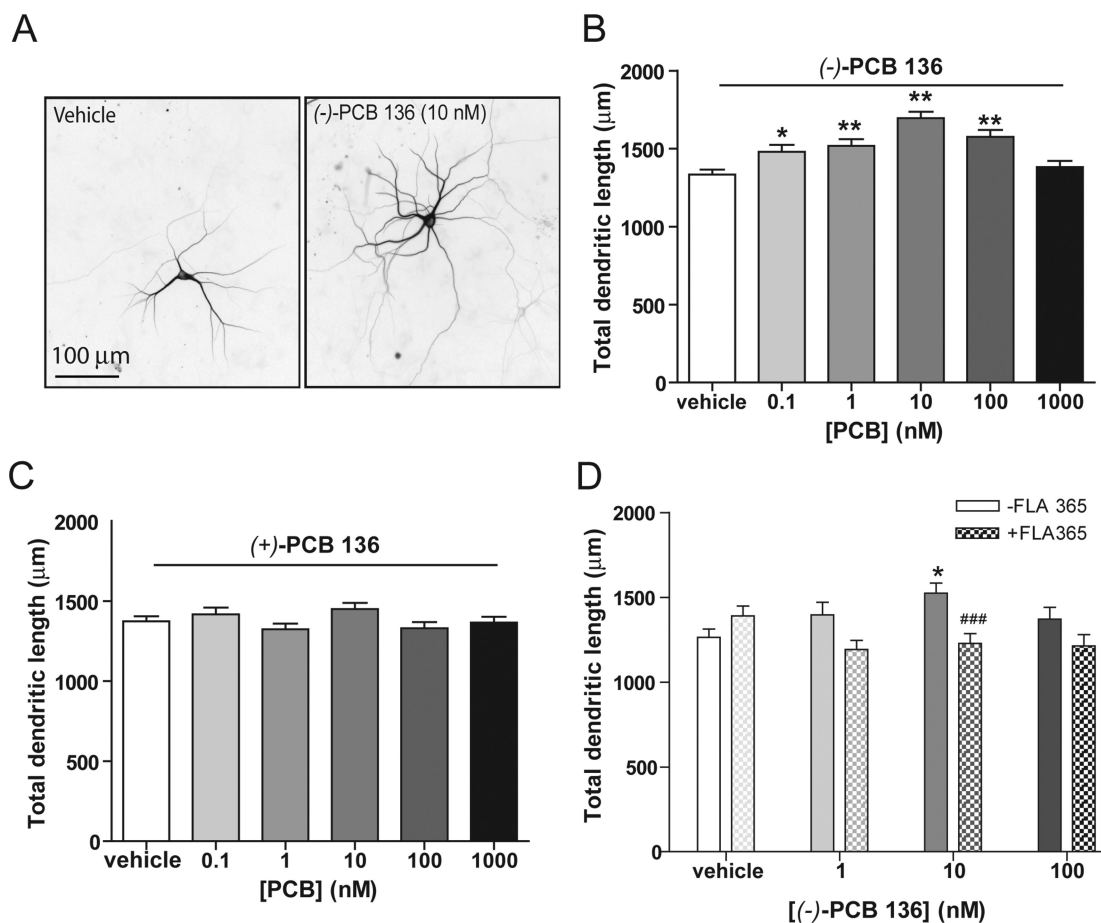
FIG. 2. Chiral PCB 136 atropselectively enhances dendritic growth in cultured hippocampal neurons. Neurons dissociated from P1 rat hippocampi were plated at high density and transfected at 6 DIV with plasmid encoding MAP2B-eGFP to visualize the dendritic arbors of individual neurons. Beginning on 7 DIV, cultures were exposed for 48 h to vehicle (DMSO diluted 1:1000 in culture medium), (−)-PCB 136 or (+)-PCB 136 at concentrations ranging from 0.1nM to 1000nM. (A) Representative photomicrographs of hippocampal neurons at 9 DIV exposed to vehicle (left) or (−)-PCB 136 at 10nM (right); bar = 100μM. (B) Quantitative analysis of dendritic length confirms that (−)-PCB 136, which sensitizes RyR, significantly enhances dendritic growth in hippocampal neurons (cumulative data from three independent dissections; $n \geq 90$ neurons per group). (C) In contrast, (+)-PCB 136, which lacks activity toward RyR, has no effect on dendritic growth. (D) The dendrite-promoting activity of (−)-PCB 136 is blocked by the specific RyR antagonist FLA365 at 10μM (data from one dissection; $n > 30$ neurons per group). *Significantly different from vehicle control at $p < 0.05$, ** $p < 0.01$, ###Significantly different from -FLA365 at same [PCB] at $p < 0.001$.

to eventually form an extensive axonal plexus that extends beyond a single microscopic field (at ×200) and overlaps significantly with that of other transfected neurons in the culture. Thus, in accordance with standard practices in developmental neuroscience for morphometric analyses of axonal growth in primary neuronal cell cultures, we examined the effect of PCB 136 atropisomers on axonal growth during the first 48 h after plating cells dissociated from P1 rat hippocampi. The axonal plexus of individual neurons was visualized by transfecting neurons with plasmids containing cDNA encoding TFP. Expression of TFP, which is distributed throughout the entire neuron, has been shown to not interfere with neuronal morphogenesis in primary cultures of hippocampal neurons (Wayman *et al.*, 2006). Exposure during the first 48 h *in vitro* to either (+)-PCB 136 or (−)-PCB 136 at concentrations ranging from 0.1 to 1000nM did not

alter the total length of the axonal arbor per neuron relative to that observed in vehicle controls (Figs. 3A and B).

It is possible that the differential effects of (−)-PCB 136 on axonal versus dendritic growth reflect differential susceptibility of immature (48 h *in vitro*) versus more mature (> 7 DIV) hippocampal cell cultures. To address this possibility, we compared the effect of (+)-PCB 136 and (−)-PCB 136 on axonal outgrowth in hippocampal neurons cultured for the same period of time as those used for the dendritic growth assays. However, as indicated above, it is technically challenging to use morphometric analyses to quantify axonal growth in mature neuronal cell cultures. Therefore, to assess the effect of PCB 136 atropisomers on axon outgrowth in mature cultures, we used Western blotting to quantify expression levels of dephosphorylated tau, a biomarker of axons (Hayashi *et al.*, 2002). This approach has been used to assess changes in axonal growth both *in vivo*
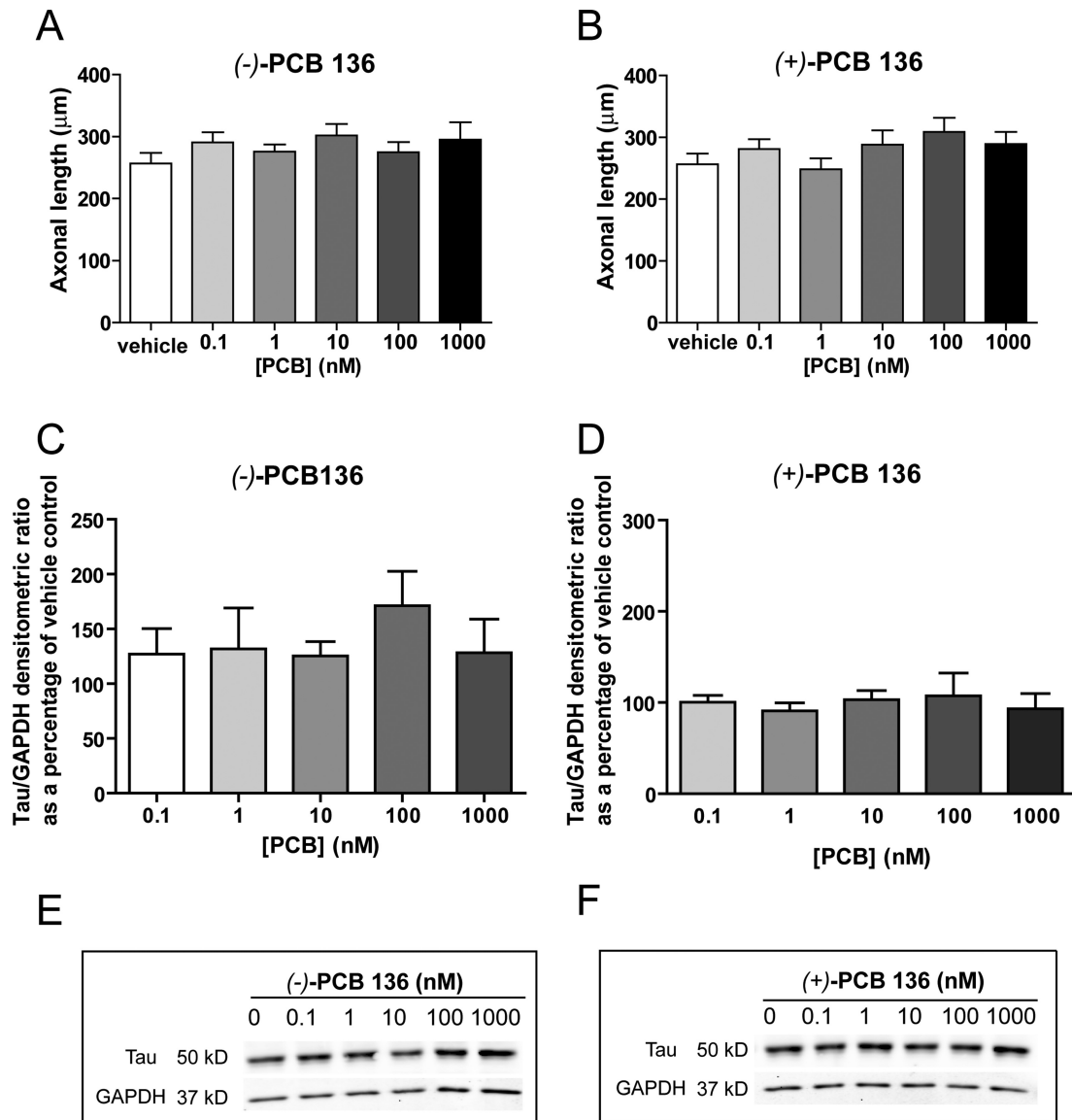
FIG. 3. PCB 136 atropisomers do not alter axonal growth in cultured hippocampal neurons. Neurons dissociated from P1 rat hippocampi were exposed to purified PCB 136 atropisomers for 48 h beginning 3 h after plating (A, B) or starting at 7 DIV (C-F). To quantify axonal growth 48 h after plating, neurons were transfected with plasmid encoding TFP 24 h after plating and cultures were imaged by fluorescence microscopy at the end of the 48 h exposure period. Under these culture conditions, neither (−)-PCB 136 (A) nor (+)-PCB 136 (B) altered axonal growth as indicated by no significant treatment-related effects on axonal length. $N \geq 30$ neurons per treatment group from one dissection. (C-F) Western blot analyses of the axonal cytoskeletal protein tau were performed to assess axonal growth in hippocampal cultures exposed to PCB 136 atropisomers from 7 to 9 DIV. Densitometric analysis revealed no significant differences in tau expression in cultures exposed to either (−)-PCB 136 (C) or (+)-PCB 136 (D) relative to cultures exposed to vehicle. $N = 3$ independent cultures. (E, F) Representative blots.

(Viberg, 2009) and *in vitro* (Chen *et al.*, 2012; Dotti *et al.*, 1987; Mundy *et al.*, 2008). A 48 h exposure to either PCB 136 atropisomer did not significantly alter levels of dephosphorylated tau at 9 DIV relative to vehicle control cultures (Figs. 3C and D).

The observation that PCB 136 atropisomers either enhance [(−)-PCB 136] or do not alter [(+)-PCB 136] dendritic growth at concentrations that have no effect on axonal growth suggests that the dendrite-promoting activity of (−)-PCB 136 is not a secondary effect of general cytotoxicity. However, to test this

possibility directly, cell viability was assessed in hippocampal cell cultures exposed to these PCB 136 atropisomers from 7 to 9 DIV. Exposure to (−)-PCB 136 or (+)-PCB 136 over the same concentration range used for the morphometric assays (0.1–1000nM) had no effect on the viability of hippocampal cell cultures relative to control cultures exposed to vehicle alone as determined by MTT reduction (Figs. 4A and B) or LDH release (Figs. 4C and D).
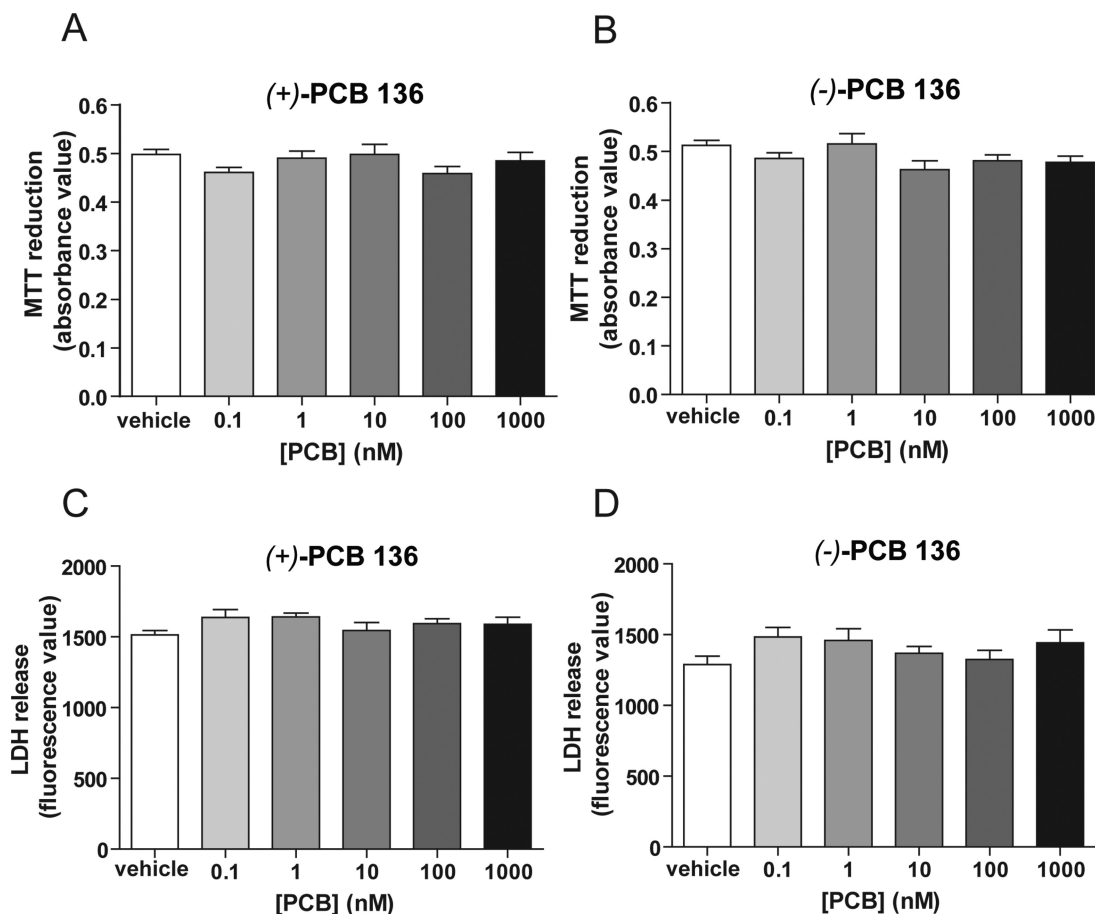
FIG. 4. Concentrations of PCB 136 that alter dendritic growth have no effect on cell viability. Neurons dissociated from P1 rat hippocampi were exposed to vehicle (DMSO diluted 1:1000 in culture medium), (−)-PCB 136 or (+)-PCB 136 at concentrations ranging from 0.1nM to 1000nM from 7 to 9 DIV. Neither (+)-PCB 136 (A, C) nor (−)-PCB 136 (B, D) had any significant effect on cell viability as determined by MTT reduction (A, B) or LDH release (C, D). $N = 12$ cultures per treatment group from three independent dissections.

Quantification of PCB 136 and Hydroxylated Metabolites in Hippocampal Cell Cultures

To assess if the atropselective effects of PCB 136 atropisomers on dendritic arborization were due to atropselective metabolism (Warner *et al.*, 2009; Wu *et al.*, 2011) or atropselective partitioning into cells, PCB 136 and its hydroxylated metabolites were quantified in the culture medium and cell pellets. PCB and metabolite levels were measured in cultures from three independent experiments that were exposed for 48 h to racemic (±)-PCB 136 or purified PCB 136 atropisomer added to the culture medium at 100nM (180 ng). Because it is not uncommon for PCBs to be retained on plastic surfaces (Pepe and Byrne, 1980), we also measured levels of PCB 136 adsorbed to the plastic cell culture plates.

Approximately 30% of the total PCB 136 added to the experiment was recovered, with 2–3% of the PCB 136 adsorbed to the plastic plates (Table 1). This observation suggests that, in agreement with other studies, a large percentage of PCB 136 is irreversibly bound to plastic surfaces. Approximately 22–26%

(1.8–2.3 ng/mg protein) of the total amount of PCB 136 remained in the medium, independent of whether (±)-, (+)-, or (−)-PCB 136 was added to the cultures (Fig. 5 and Table 1). PCB levels associated with the cell pellets ranged from 3.3 to 3.8 ng/mg protein in cultures exposed to (±)-, (+)-, or (−)-PCB 136, which corresponds to approximately 2% of the total amount of PCB 136. No hydroxylated metabolites were detected in the medium or the cell pellet.

Because it has previously been reported that the uptake of PCBs by cells in culture depends on the protein concentration in the cell culture medium (Mangelsdorf *et al.*, 1987), we also determined the protein adjusted medium-to-cell ratio, which ranged from 0.49 to 0.62 (Table 1). The medium-to-cell ratio of PCB 136 showed no significant difference between cultures exposed to racemic (±)-PCB 136, purified (+)-PCB 136, or purified (−)-PCB 136 (Fig. 5 and Table 1). Similarly, the enantiomeric fractions of (±)-PCB 136, a measure of its atropisomeric enrichment, were near racemic in both medium and cell pellets.

TABLE 1.

Quantification of PCB 136 Atropisomers in Cell Media and Cell Pellets of Hippocampal Neurons Exposed *In Vitro* to Racemic (±) PCB 136 or Purified PCB 136 Atropisomers at 100nM from 7 to 9 DIV

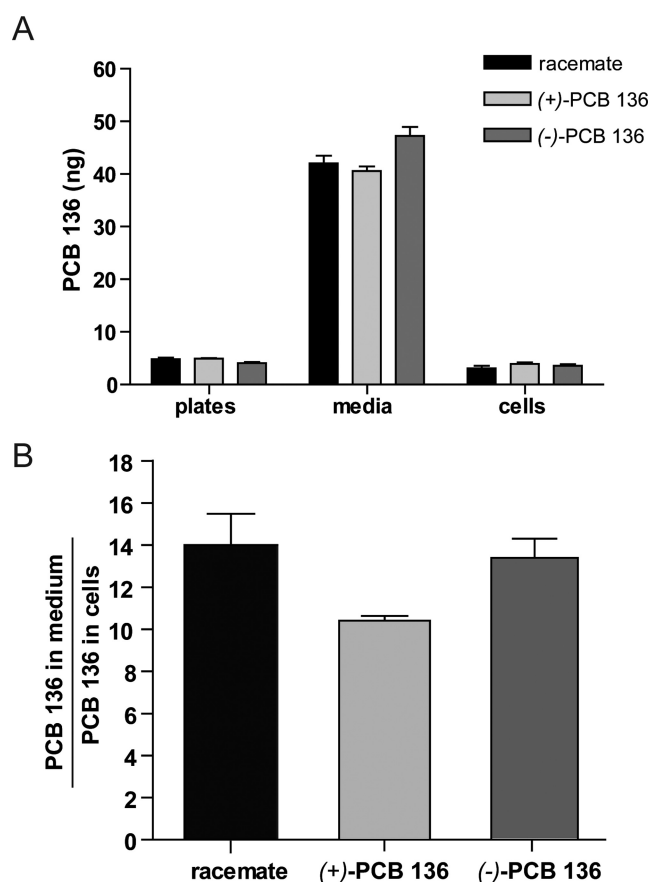| Compound to which cell cultures were exposed	Medium	Cells	Medium-to-cell ratio
PCB 136 levels [ng in sample]			
(±)-PCB 136	42.0 ± 2.7	3.1 ± 0.8	14.0 ± 3.0
(+)-PCB 136	40.6 ± 1.8	3.9 ± 0.3	10.3 ± 0.3
(−)-PCB 136	47.2 ± 3.3	3.6 ± 0.3	13.3 ± 2.2
PCB 136 concentration [ng/mg protein]			
(±)-PCB 136	1.9 ± 0.1	3.3 ± 1.2	0.61 ± 0.18
(+)-PCB 136	1.8 ± 0.1	3.6 ± 0.7	0.49 ± 0.07
(−)- PCB 136	2.3 ± 0.2	3.8 ± 0.5	0.63 ± 0.16

FIG. 5. Quantification of PCB 136 in cell media and cell pellets shows no atropselective partitioning of PCB 136 into cells. Neurons dissociated from P1 rat hippocampi were exposed to racemic PCB 136 mixture or to purified (−)-PCB 136 or (+)-PCB 136 atropisomers at 100nM from 7 to 9 DIV. (A) As determined by gas chromatography, the amount of PCB 136 adsorbed to tissue culture plastic in the medium and in cell pellet was similar across all PCB 136 treatment groups. (B) Similarly, the ratio of PCB 136 in the medium to the cell pellet was not significantly different between cultures exposed to different PC 136 treatments. $N = 3$ independent dissections per treatment group.

Atropselective Effects of PCB136 on Functional Parameters of Neuronal Connectivity

We previously reported that PCB 95 promotes dendritic growth in cultured hippocampal neurons by increasing the frequency of intracellular Ca^{2+} oscillations downstream of RyR activation (Wayman *et al.*, 2012a). Because the atropselective effects of PCB 136 on dendritic growth are dependent on RyR activity (Fig. 2D), we predicted that PCB 136 would exert atropselective effects on neuronal Ca^{2+} signaling. To test this prediction, we used real-time Ca^{2+} imaging techniques to examine Ca^{2+} oscillatory behavior in neurons. Cultured hippocampal neurons that had not previously been exposed to PCBs were loaded with the Ca^{2+}-sensitive dye Fluo-4 at 7 DIV immediately before focal applications of vehicle, (−)-PCB 136 or (+)-PCB 136. Relative to cultures exposed to vehicle, acute application of (−)-PCB 136 at 200nM, a concentration that promotes robust dendritic growth (data not shown), significantly increased the frequency of Ca^{2+} oscillations in both soma and distal dendrites of hippocampal neurons (Fig. 6). In contrast, acute exposure to the same concentration of (+)-PCB 136 had no significant effect on the frequency of Ca^{2+} oscillations in either soma or distal dendrites (Fig. 6).

Next, we tested whether PCB 136 atropisomers atropselectively influence spontaneous electrical spiking activity of hippocampal neurons cultured on MEA probes (Fig. 7A). Spontaneous spike (action potential) activity can be detected in these cultures by 21 DIV as illustrated by spike trains collected from 21 DIV cultures exposed to vehicle (Fig. 7B). Acute sequential exposure to increasing concentrations of (−)-PCB 136 at 10 min intervals significantly increased the number of spontaneous spikes, whereas exposure to the same concentrations of (+)-PCB 136 did not alter spike activity relative to vehicle controls (Figs. 7B–D). Although increased spike activity was observed at concentrations of (−)-PCB 136 ≥ 2nM, post hoc analyses indicated that statistically significant increases in spike activity occurred at (−)-PCB 136 concentrations of 20 and 2000nM (Figs. 7B–D).
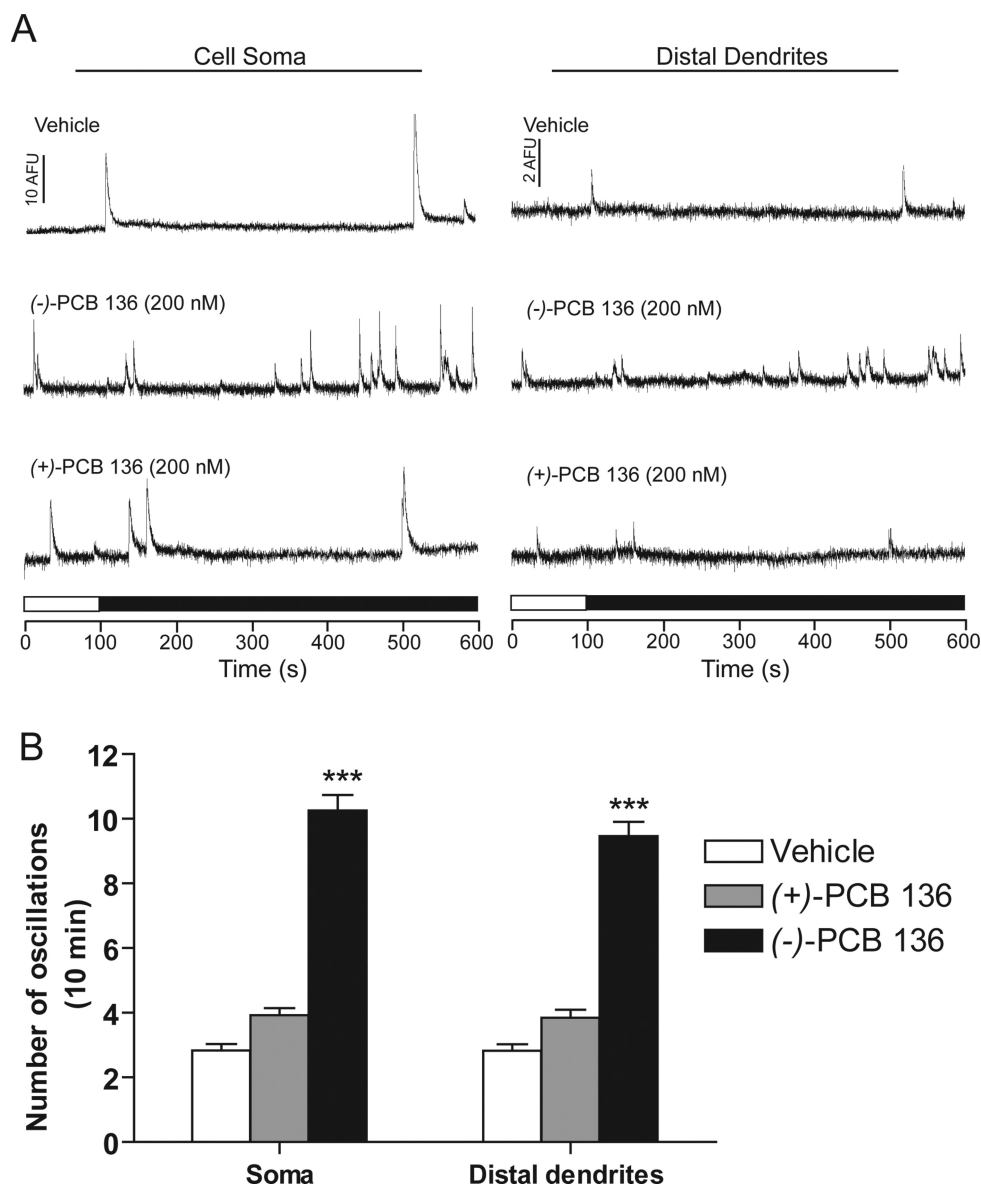
FIG. 6. Acute exposure to (−)-PCB 136 but not (+)-PCB 136 increases the frequency of Ca^{2+} oscillations. Primary dissociated rat hippocampal neurons (7 DIV) were loaded with Fluo-4. After establishing the baseline, cells were perfused with imaging buffer containing either (−)-PCB 136 or (+)-PCB 136 (200nM) or an equivalent volume of DMSO (vehicle control). (A) Representative Ca^{2+} oscillations acquired from the soma and distal dendrites of neurons exposed to vehicle or purified PCB 136 atropisomers. (B) Quantification of the frequency of spontaneous Ca^{2+} transients ≥ 2 times the mean normalized baseline fluorescence in the soma and distal dendrites. $N = 10$–12 neurons per treatment group from two independent cultures; ***significantly different from vehicle control at $p < 0.001$.

DISCUSSION

We previously reported that PCB 95, a chiral congener, promotes dendritic growth in hippocampal neurons via RyR-dependent stimulation of Ca^{2+} signaling pathways (Wayman *et al.*, 2012a,b). Here, we demonstrate that these effects can be generalized to another chiral congener, PCB 136. More importantly, we provide the first evidence of an atropselective effect of an environmentally relevant PCB on specific neurodevelopmental endpoints of relevance to human health (Stamou *et al.*,

2013). Specifically, we demonstrate that (−)-PCB 136, but not (+)-PCB 136, enhances dendritic arborization in cultured hippocampal neurons. As observed with racemic PCB 95 (Wayman *et al.*, 2012b), the dendrite-promoting activity of (−)-PCB 136 exhibits a non-monotonic concentration-response relationship. This does not reflect cytotoxicity at higher concentrations because (−)-PCB 136 did not alter MTT reduction or LDH release at any of the concentrations used in the dendritic assays. MTT reduction or LDH release were also not affected by similar concentrations of (+)-PCB 136, indicating that general cytotoxicity
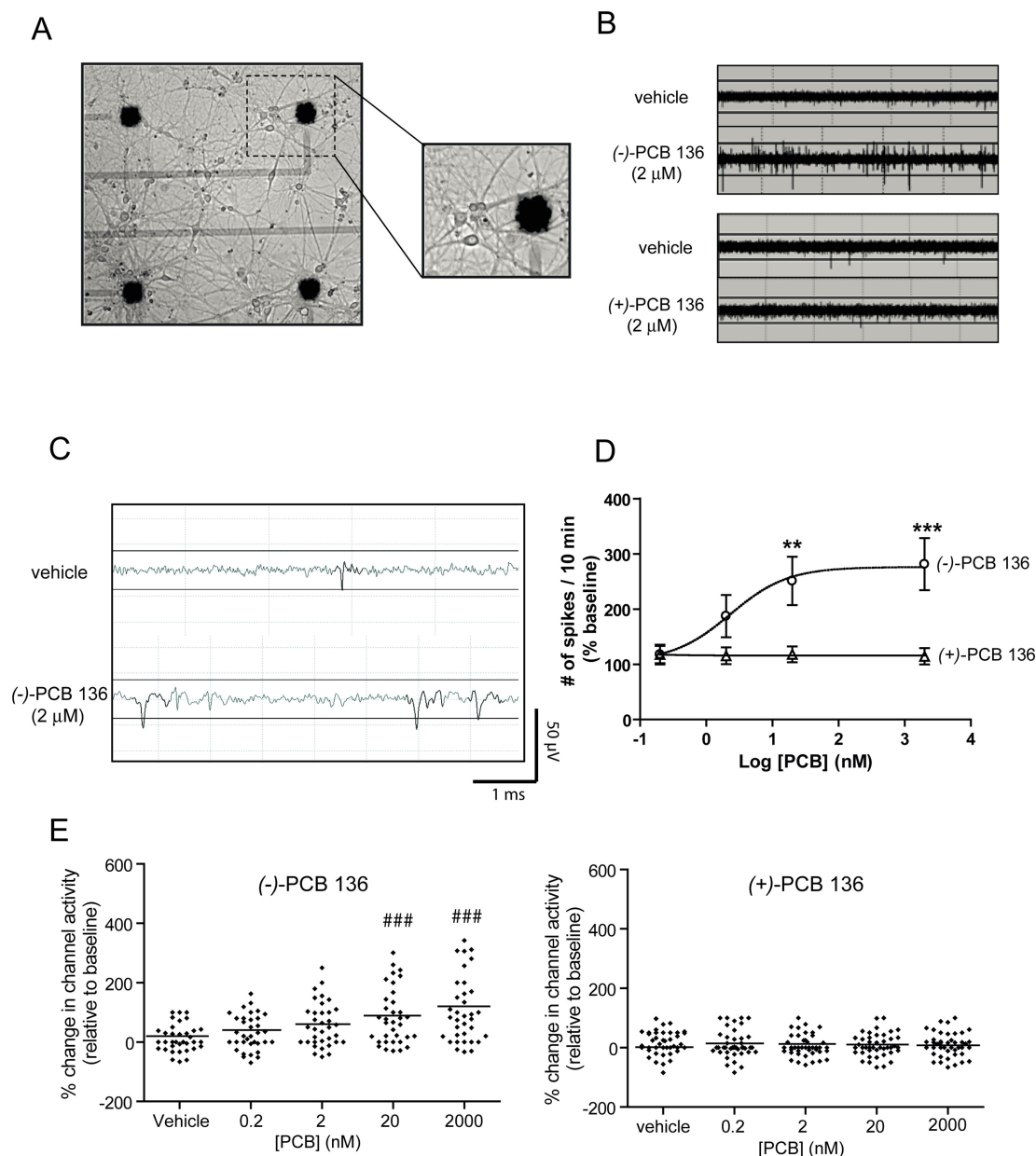
FIG. 7. PCB 136 atropselectively enhances spontaneous activity in hippocampal neurons cultured on microelectrode arrays (MEAs). Neurons dissociated from P1 rat hippocampi were plated on MEAs precoated with poly-L-lysine and laminin. Activity was recorded in 21 DIV cultures acutely exposed sequentially to vehicle (DMSO) and increasing concentrations of one of the PCB 136 atropisomers. (A) Representative photomicrograph of a 21 DIV hippocampal culture illustrating the distribution of neuronal cell bodies and neurites in relationship to the electrodes (solid black circles). (B) Representative spike trains over a 6-s period in neurons exposed acutely to (−)-PCB 136 or (+)-PCB 136. (C) Representative trace of spontaneous activity in cultured neurons exposed to vehicle or (−)-PCB 136 over a 5 ms period. Signals that exceeded a threshold of ±15 μV (solid line) were scored as a spike. (D) Analysis of spike activity of active electrodes indicates that (−)-PCB 136 but not (+)-PCB 136 increases spontaneous spike activity in a concentration-dependent manner. Each electrode is normalized to its own baseline. $N = 3$ arrays per treatment group from three independent dissections. **Statistically different from baseline at $p < 0.01$; *** $p < 0.001$ (ANOVA with *post hoc* Tukey's test). (D) Whisker plots illustrating the percent change in the number of active electrodes within the MEA (e.g., channel activity) in response to vehicle or varying concentrations of (−)-PCB 136 (left panel) or (+)-PCB 136 (right panel). The horizontal line within each treatment represents the mean value at each PCB 136 concentration. ###Statistically different from baseline at $p < 0.001$.

is not the reason for the lack of a dendritic response to this atropisomer.

Three lines of evidence indicate that the atropselective effects of PCB 136 on dendritic arborization are mediated by atropselective interactions with RyRs. First, the dendrite-promoting activity of PCB 136 exhibits the same atropisomeric specificity as its effects on RyR activity (Pessah *et al.*, 2009). Second, (−)-PCB 136-induced dendritic growth is blocked by pharmacological blockade of RyR activity with FLA 365 (Chiesi *et al.*, 1988; Mack *et al.*, 1992). Third, we previously demonstrated that PCB 95 promotes dendritic growth via RyR-dependent increases in spontaneous Ca^{2+} oscillations (Wayman *et al.*, 2012a,b). Here, we show that (−)-PCB 136, but not (+)-PCB 136, increases spontaneous Ca^{2+} oscillations in the soma and dendrites of hippocampal neurons. Collectively, these data support a model in which atropselective interactions of PCB 136 with RyR translate into atropselective activation of Ca^{2+}-dependent mechanisms of dendritic growth.

PCB 136 also atropselectively increased neuronal activity in hippocampal neurons. This is consistent with evidence that RyR activity influences neuronal excitability (Pessah *et al.*, 2010), and indicates that chiral PCBs influence not only morphometric but also functional parameters of neuronal connectivity via atropselective interactions with RyRs. The concentration-response relationship of (−)-PCB 136 effects on neuronal activity differs from that of its effects on dendritic arborization, suggesting dissociation between these two effects. However, this interpretation is complicated by differences between assays of these endpoints with respect to length of exposure and age of the cultures at the time of exposure. Dendritic growth was studied in cultures exposed to PCB 136 atropisomers for 48 h starting on DIV 7, whereas neuronal activity studies were performed using 21 DIV cultures exposed acutely to PCB 136 atropisomers. Whether these two effects of (−)-PCB 136 are causally linked remains to be established but is suggested by extensive literature linking neuronal activity to changes in dendritic arborization (Cline, 2001). PCBs have been reported to modulate other receptors and ion channels that influence neuronal activity, specifically the $GABA_A$ receptor and nicotinic acetylcholine receptors (Fernandes *et al.*, 2010; Hendriks *et al.*, 2010), suggesting that RyR-independent mechanisms may also contribute to the effects of (−)-PCB 136 on neuronal activity. Thus, in a heterologous *Xenopus* oocyte expression system, NDL PCBs act as full or partial agonists of the $GABA_A$ receptor and as antagonists of the $\alpha_4\beta_2$ nicotinic acetylcholine receptor (Fernandes *et al.*, 2010; Hendriks *et al.*, 2010). Whether NDL PCBs similarly modulate native $GABA_A$ and nicotinic acetylcholine receptors in neurons has yet to be established, but even if this proves to be the case, it is not clear how these effects would contribute to the increased spike activity observed in neurons exposed to (−)-PCB 136 because activation of $GABA_A$ receptors and/or inhibition of nicotinic acetylcholine receptors would be expected to dampen neuronal excitability.

The finding that PCB 136 effects on dendritic growth, spontaneous Ca^{2+} oscillations, and neuronal activity exhibit the same atropisomeric specificity as its effects on RyR activity identify RyRs as primary molecular targets in the adverse outcome pathway of chiral PCB developmental neurotoxicity. This also suggests that parameters of neuronal form and function influenced by RyR activity are likely to be modulated by RyR-active PCBs. Thus, it was surprising that (−)-PCB 136 had no effect on axonal growth because RyR activity has been implicated in controlling axonal growth and guidance (Ooashi *et al.*, 2005; Welshhans and Rehder, 2007). Differential RyR expression profiles between neuronal cell types may explain this apparent discrepancy. Although all three RyR isoforms are expressed in the brain, they are differentially distributed among specific brain regions, cell types, and cellular regions, reflecting their participation in specialized functions (Pessah *et al.*, 2010). Of the two studies reporting a role for RyR in axonal growth, one did not identify the RyR isoform(s) mediating nitric oxide effects on axonal growth in *Heliosoma* BV neurons (Welshhans and Rehder, 2007); but the other identified RyR3 as the isoform mediating the influence of cell adhesion molecules on axonal growth in rat dorsal root ganglion neurons (Ooashi *et al.*, 2005). RyR3 is expressed at low levels in the developing hippocampus (Pessah *et al.*, 2010), but we were not able to detect RyR3 in our hippocampal cultures by Western blotting (Wayman *et al.*, 2012b). This suggests that the reason (−)-PCB 136 had no effect on axonal growth in our cultures is because the neurons do not express RyR3. Thus, neurodevelopmental outcome following exposure to RyR-active PCBs will likely depend in part on the RyR expression profile of the exposed cell.

Another mechanism potentially contributing to the atropselective developmental neurotoxicity of PCB 136 is atropselective metabolism and/or cellular uptake. PCB 136 can be metabolized atropselectively to hydroxylated metabolites by hepatic cytochrome P450 (CYP) 2B enzymes, such as CYP 2B1 (Waller *et al.*, 1999; Warner *et al.*, 2009; Wu *et al.*, 2011), and these metabolites can be equally or more potent than the parent compound with respect to RyR sensitization (Niknam *et al.*, 2013). PCB 136 has been detected in brain tissue (Kania-Korwel *et al.*, 2010), and CYP 2B1 is active in rat brain (Miksys and Tyndale, 2009). However, we did not detect hydroxylated metabolites in cell pellets or media from hippocampal cell cultures exposed to racemic PCB 136 or purified atropisomers, which is consistent with previous studies in hippocampal slice cultures (Wu *et al.*, 2013). It is unknown if this is because our cultures cannot metabolize PCB 136 under the culture conditions used for these studies or if the levels of hydroxylated metabolites were below the detection limit (0.04–0.22 ng) of our analytical method (GC-ECD). In support of the latter, the activity of rat CYP 2B1 in microsomes derived from the hippocampus, while comparable to the whole brain, is about 20 times lower than CYP 2B1 activity in liver microsomes (Dhawan *et al.*, 1999). Although the influence of atropselective metabolism in the brain on the developmental neurotoxicity of chiral PCBs remains unknown,

our findings suggest that atropselective metabolism is not a significant mechanism contributing to the atropselective effects of PCB 136 in cultured hippocampal neurons.

We also ruled out atropselective cellular uptake as contributing to atropselective effects of PCB 136 *in vitro*. Quantification of the parent congener in hippocampal cell cultures exposed from 7–9 DIV to racemic PCB or purified atropisomers showed that the medium-to-cell ratio of PCB 136 did not differ significantly between treatment groups. Similarly, the enantiomeric fractions of (±)-PCB 136 in medium and cell pellets were near racemic. Collectively, these observations indicate that the partitioning of PCB 136 atropisomers between medium and cells is not atropselective. Our analysis also revealed that the largest percentage of PCB 136 remained in the cell culture medium as indicated by a medium-to-cell ratio of 5.4 ± 1.4. However, the protein adjusted medium-to-cell ratio ranged from 0.49 to 0.62, indicating a preferential partitioning of PCB 136 atropisomers into the cells under the conditions employed in our study. Average PCB 136 levels in hippocampal cells were 9.4 ± 2.0 ng PCB 136 per 10^6 cells, which is approximately 2% of PCB added to the cultures. This is in marked contrast to previous reports of intracellular levels of PCBs 5–40-fold greater than the original solution in primary hippocampal slice cultures or dissociated cultures of rat cortical neurons (Meacham *et al.*, 2005; Mundy *et al.*, 2004). However, our findings are consistent with other cell culture studies that report only a small percentage (1.5–35%) of the PCBs added to media associated with the cell pellet (Byrne and Pepe, 1981; Mangelsdorf *et al.*, 1987; Shain *et al.*, 1991). The reason for the discrepancies between these studies is unknown but likely reflects differences in cell types, culture conditions and method of detection.

Although we did not observe atropselective uptake of PCB 136 into cultured hippocampal neurons, emerging evidence suggests significant potential for atropisomeric enrichment of PCBs in some individuals and/or human populations (Lehmler *et al.*, 2010). Our experimental evidence that PCB 136 atropselectively modulates critical neurodevelopmental processes suggests that variable atropisomeric enrichment influences risk for adverse neurodevelopmental outcomes following PCB exposure. The public health relevance of this risk is underscored by data documenting significant human exposure to chiral PCBs (Lehmler *et al.*, 2010; Marek *et al.*, 2013; Megson *et al.*, 2013; Thompson and Boekelheide, 2013), and by our observation that the concentration range over which (−)-PCB 136 altered dendritic growth corresponds to 0.04–36 ng/g, which is comparable to the levels of chiral PCBs reported in human blood (0.03–98 ng/g) (Bi *et al.*, 2007; Bloom *et al.*, 2005; DeCaprio *et al.*, 2005; Gerstenberger *et al.*, 2000; Jursa *et al.*, 2006; Park *et al.*, 2007; Schaeffer *et al.*, 2006; Schell *et al.*, 2003; Turci *et al.*, 2006). Given that atropisomeric enrichment of chiral PCBs likely results from atropselective metabolism by cytochrome P450s (Warner *et al.*, 2009; Wu *et al.*, 2011), our findings suggest that not only RyR polymorphisms (Pessah *et al.*, 2010) but also cytochrome P450 polymorphisms may be important genetic susceptibility factors influencing PCB developmental neurotoxicity.

REFERENCES

Bi, X., Thomas, G. O., Jones, K. C., Qu, W., Sheng, G., Martin, F. L., and Fu, J. (2007). Exposure of electronics dismantling workers to polybrominated diphenyl ethers, polychlorinated biphenyls, and organochlorine pesticides in South China. *Environ. Sci. Technol.* **41**, 5647–5653.

Bloom, M. S., Vena, J. E., Swanson, M. K., Moysich, K. B., and Olson, J. R. (2005). Profiles of ortho-polychlorinated biphenyl congeners, dichlorodiphenyldichloroethylene, hexachlorobenzene, and Mirex among male Lake Ontario sportfish consumers: The New York State Angler cohort study. *Environ. Res.* **97**, 178–194.

Boucher, O., Muckle, G., and Bastien, C. H. (2009). Prenatal exposure to polychlorinated biphenyls: A neuropsychologic analysis. *Environ. Health Perspect.* **117**, 7–16.

Byrne, J. J.,, and Pepe, M. G. (1981). A protein binding radio-assay method for measuring PCB (hexachlorobiphenyl) incorporation in culture cells. *Bull. Environ. Contam. Toxicol.* **26**, 237–242.

Carpenter, D. O. (2006). Polychlorinated biphenyls (PCBs): Routes of exposure and effects on human health. *Rev. Environ. Health* **21**, 1–23.

Chen, Q., Zhou, Z., Zhang, L., Wang, Y., Zhang, Y. W., Zhong, M., Xu, S. C., Chen, C. H., Li, L., and Yu, Z. P. (2012). Tau protein is involved in morphological plasticity in hippocampal neurons in response to BDNF. *Neurochem. Int.* **60**, 233–242.

Chiesi, M., Schwaller, R., and Calviello, G. (1988). Inhibition of rapid Ca-release from isolated skeletal and cardiac sarcoplasmic reticulum (SR) membranes. *Biochem. Biophys. Res. Commun.* **154**, 1–8.

Cline, H. T. (2001). Dendritic arbor development and synaptogenesis. *Curr. Opin. Neurobiol.* **11**, 118–126.

DeCaprio, A. P., Johnson, G. W., Tarbell, A. M., Carpenter, D. O., Chiarenzelli, J. R., Morse, G. S., Santiago-Rivera, A. L., and Schymura, M. J. (2005). Polychlorinated biphenyl (PCB) exposure assessment by multivariate statistical analysis of serum congener profiles in an adult Native American population. *Environ. Res.* **98**, 284–302.

Dhawan, A., Parmar, D., Dayal, M., and Seth, P. K. (1999). Cytochrome P450 (P450) isoenzyme specific dealkylation of alkoxyresorufins in rat brain microsomes. *Mol. Cell. Biochem.* **200**, 169–176.

Dotti, C. G., Banker, G. A., and Binder, L. I. (1987). The expression and distribution of the microtubule-associated proteins tau and microtubule-associated protein 2 in hippocampal neurons in the rat in situ and in cell culture. *Neuroscience* **23**, 121–130.

Fernandes, E. C., Hendriks, H. S., van Kleef, R. G., Reniers, A., Andersson, P. L., van den Berg, M., and Westerink, R. H. (2010). Activation and potentiation of human GABAA receptors by non-dioxin-like PCBs depends on chlorination pattern. *Toxicol. Sci.* **118**, 183–190.

Gerstenberger, S. L., Dellinger, J. A., and Hansen, L. G. (2000). Concentrations and frequencies of polychlorinated biphenyl congeners in a Native American population that consumes Great Lakes fish. *J. Toxicol. Clin. Toxicol.* **38**, 729–746.

Hayashi, K., Kawai-Hirai, R., Ishikawa, K., and Takata, K. (2002). Reversal of neuronal polarity characterized by conversion of dendrites into axons in neonatal rat cortical neurons in vitro. *Neuroscience* **110**, 7–17.

Hendriks, H. S., Antunes Fernandes, E. C., Bergman, A., van den Berg, M., and Westerink, R. H. (2010). PCB-47, PBDE-47, and 6-OH-PBDE-47 differentially modulate human GABAA and alpha4beta2 nicotinic acetylcholine receptors. *Toxicol. Sci.* **118**, 635–642.

Hertle, D. N., and Yeckel, M. F. (2007). Distribution of inositol-1,4,5-trisphosphate receptor isotypes and ryanodine receptor isotypes during maturation of the rat hippocampus. *Neuroscience* **150**, 625–638.

Hornbuckle, K. C., Carlson, D. L., Swackhamer, D. L., Baker, J. E., and Eisenreich, S. J. (2006). Polychlorinated Biphenyls in the Great Lakes. In *The Handbook of Environmental Chemistry: Persistent Organic Pollutants in the Great Lakes* (R. Hites, Ed.), Vol. **5**, pp. 13–70. Springer-Verlag, Berlin.

Hu, D., and Hornbuckle, K. C. (2010). Inadvertent polychlorinated biphenyls in commercial paint pigments. *Environ. Sci. Technol.* **44**, 2822–2827.

Hwang, H. M., Green, P. G., and Young, T. M. (2006). Tidal salt marsh sediment in California, USA. Part 1: Occurrence and sources of organic contaminants. *Chemosphere* **64**, 1383–1392.

Jamshidi, A., Hunter, S., Hazrati, S., and Harrad, S. (2007). Concentrations and chiral signatures of polychlorinated biphenyls in outdoor and indoor air and soil in a major U.K. conurbation. *Environ. Sci. Technol.* **41**, 2153–2158.

Jursa, S., Chovancova, J., Petrik, J., and Loksa, J. (2006). Dioxin-like and non-dioxin-like PCBs in human serum of Slovak population. *Chemosphere* **64**, 686–691.

Kania-Korwel, I., El-Komy, M. H., Veng-Pedersen, P., and Lehmler, H. J. (2010). Clearance of polychlorinated biphenyl atropisomers is enantioselective in female C57Bl/6 mice. *Environ. Sci. Technol.* **44**, 2828–2835.

Kania-Korwel, I., Hrycay, E. G., Bandiera, S., and Lehmler, H.-J. (2008). 2,2′,3,3′,6,6′-Hexachlorobiphenyl (PCB 136) atropisomers interact enantioselectively with hepatic microsomal cytochrome P450 enzymes. *Chem. Res. Toxicol.* **21**, 1295–1303.

Kenet, T., Froemke, R. C., Schreiner, C. E., Pessah, I. N., and Merzenich, M. M. (2007). Perinatal exposure to a noncoplanar polychlorinated biphenyl alters tonotopy, receptive fields, and plasticity in rat primary auditory cortex. *Proc. Natl. Acad. Sci. U.S.A.* **104**, 7646–7651.

Korrick, S. A., and Sagiv, S. K. (2008). Polychlorinated biphenyls, organochlorine pesticides and neurodevelopment. *Curr. Opin. Pediatr.* **20**, 198–204.

Kostyniak, P. J., Hansen, L. G., Widholm, J. J., Fitzpatrick, R. D., Olson, J. R., Helferich, J. L., Kim, K. H., Sable, H. J., Seegal, R. F., Pessah, I. N., et al. (2005). Formulation and characterization of an experimental PCB mixture designed to mimic human exposure from contaminated fish. *Toxicol. Sci.* **88**, 400–411.

Landrigan, P. J., Lambertini, L., and Birnbaum, L. S. (2012). A research strategy to discover the environmental causes of autism and neurodevelopmental disabilities. *Environ. Health Perspect.* **120**, a258–a260.

Lehmler, H. J., Harrad, S. J., Huhnerfuss, H., Kania-Korwel, I., Lee, C. M., Lu, Z., and Wong, C. S. (2010). Chiral polychlorinated biphenyl transport, metabolism, and distribution: A review. *Environ. Sci. Technol.* **44**, 2757–2766.

Mack, W. M., Zimanyi, I., and Pessah, I. N. (1992). Discrimination of multiple binding sites for antagonists of the calcium release channel complex of skeletal and cardiac sarcoplasmic reticulum. *J. Pharmacol. Exp. Ther.* **262**, 1028–1037.

Mangelsdorf, I., Buff, K., and Berndt, J. (1987). Uptake of persistent environmental chemicals by cultured human cells. *Biochem. Pharmacol.* **36**, 2071–2078.

Marek, R. F., Thorne, P. S., Wang, K., Dewall, J., and Hornbuckle, K. C. (2013). PCBs and OH-PCBs in serum from children and mothers in urban and rural U.S. communities. *Environ. Sci. Technol.* **47**, 3353–3361.

Martinez, A., and Hornbuckle, K. C. (2011). Record of PCB congeners, sorbents and potential toxicity in core samples in Indiana Harbor and Ship Canal. *Chemosphere* **85**, 542–547.

Meacham, C. A., Freudenrich, T. M., Anderson, W. L., Sui, L., Lyons-Darden, T., Barone, S., Jr, Gilbert, M. E., Mundy, W. R., and Shafer, T. J. (2005). Accumulation of methylmercury or polychlorinated biphenyls in in vitro models of rat neuronal tissue. *Toxicol. Appl. Pharmacol.* **205**, 177–187.

Megson, D., O'Sullivan, G., Comber, S., Worsfold, P. J., Lohan, M. C., Edwards, M. R., Shields, W. J., Sandau, C. D., and Patterson, D. G., Jr (2013). Elucidating the structural properties that influence the persistence of PCBs in humans using the National Health and Nutrition Examination Survey (NHANES) dataset. *Sci. Total Environ.* **461**, 99–107.

Meijering, E., Jacob, M., Sarria, J. C., Steiner, P., Hirling, H., and Unser, M. (2004). Design and validation of a tool for neurite tracing and analysis in fluorescence microscopy images. *Cytometry A* **58**, 167–176.

Miksys, S., and Tyndale, R. (2009). Brain drug-metabolizing cytochrome P450 enzymes are active in vivo, demonstrated by mechanism-based enzyme inhibition. *Neuropsychopharmacology* **34**, 634–640.

Mundy, W. R., Freudenrich, T. M., Crofton, K. M., and DeVito, M. J. (2004). Accumulation of PBDE-47 in primary cultures of rat neocortical cells. *Toxicol. Sci.* **82**, 164–169.

Mundy, W. R., Robinette, B., Radio, N. M., and Freudenrich, T. M. (2008). Protein biomarkers associated with growth and synaptogenesis in a cell culture model of neuronal development. *Toxicology* **249**, 220–229.

Niknam, Y., Feng, W., Cherednichenko, G., Dong, Y., Joshi, S. N., Vyas, S. M., Lehmler, H. J., and Pessah, I. N. (2013). Structure-activity relationship of selected meta- and para-hydroxylated non-dioxin-like polychlorinated biphenyls: from single RyR1 channels to muscle dysfunction. *Toxicol. Sci.* **136**, 500–513.

Ooashi, N., Futatsugi, A., Yoshihara, F., Mikoshiba, K., and Kamiguchi, H. (2005). Cell adhesion molecules regulate Ca2+-mediated steering of growth cones via cyclic AMP and ryanodine receptor type 3. *J. Cell Biol.* **170**, 1159–1167.

Park, H., Lee, S. J., Kang, J. H., and Chang, Y. S. (2007). Congener-specific approach to human PCB concentrations by serum analysis. *Chemosphere* **68**, 1699–1706.

Pepe, M. G., and Byrne, J. J. (1980). Adhesion-binding of 2,2′,4,4′,5,5′-hexachlorobiphenyl to glass and plastic: A possible source of error for PCB analysis. *Bull. Environ. Contam. Toxicol.* **25**, 936–940.

Pessah, I. N., Cherednichenko, G., and Lein, P. J. (2010). Minding the calcium store: Ryanodine receptor activation as a convergent mechanism of PCB toxicity. *Pharmacol. Ther.* **125**, 260–285.

Pessah, I. N., Lehmler, H. J., Robertson, L. W., Perez, C. F., Cabrales, E., Bose, D. D., and Feng, W. (2009). Enantiomeric specificity of (-)-2,2′,3,3′,6,6′-hexachlorobiphenyl toward ryanodine receptor types 1 and 2. *Chem. Res. Toxicol.* **22**, 201–207.

Robinette, B. L., Harrill, J. A., Mundy, W. R., and Shafer, T. J. (2011). In vitro assessment of developmental neurotoxicity: Use of microelectrode arrays to measure functional changes in neuronal network ontogeny. *Front. Neuroeng.* **4**, 1.

Schaeffer, D. J., Dellinger, J. A., Needham, L. L., and Hansen, L. G. (2006). Serum PCB profiles in Native Americans from Wisconsin based on region, diet, age, and gender: Implications for epidemiology studies. *Sci. Total Environ.* **357**, 74–87.

Schantz, S. L., Gardiner, J. C., Aguiar, A., Tang, X., Gasior, D. M., Sweeney, A. M., Peck, J. D., Gillard, D., and Kostyniak, P. J. (2010). Contaminant profiles in Southeast Asian immigrants consuming fish from polluted waters in northeastern Wisconsin. *Environ. Res.* **110**, 33–39.

Schantz, S. L., Seo, B. W., Wong, P. W., and Pessah, I. N. (1997). Long-term effects of developmental exposure to 2,2′,3,5′,6- pentachlorobiphenyl (PCB 95) on locomotor activity, spatial learning and memory and brain ryanodine binding. *Neurotoxicology* **18**, 457–467.

Schantz, S. L., Widholm, J. J., and Rice, D. C. (2003). Effects of PCB exposure on neuropsychological function in children. *Environ. Health Perspect.* **111**, 357–576.

Schell, L. M., Hubicki, L. A., DeCaprio, A. P., Gallo, M. V., Ravenscroft, J., Tarbell, A., Jacobs, A., David, D., and Worswick, P. (2003). Organochlorines, lead, and mercury in Akwesasne Mohawk youth. *Environ. Health Perspect.* **111**, 954–961.

Seymour-Laurent, K. J., and Barish, M. E. (1995). Inositol 1,4,5-trisphosphate and ryanodine receptor distributions and patterns of acetylcholine- and caffeine-induced calcium release in cultured mouse hippocampal neurons. *J. Neurosci.* **15**, 2592–2608.

Shain, W., Bush, B., and Seegal, R. (1991). Neurotoxicity of polychlorinated biphenyls: Structure-activity relationship of individual congeners. *Toxicol. Appl. Pharmacol.* **111**, 33–42.

Stamou, M., Streifel, K. M., Goines, P. E., and Lein, P. J. (2013). Neuronal connectivity as a convergent target of gene x environment interactions that confer risk for Autism Spectrum Disorders. *Neurotoxicol. Teratol.* **36**, 3–16.

Thomas, K., Xue, J., Williams, R., Jones, P., and Whitaker, D. (2012). *Polychlorinated biphenyls (PCBs) in School Buildings: Sources, Environmental Levels and Exposures*. Unites StatesEnviron mental Protection Agency. Report EPA/600/R-12/051,150 pages.

Thompson, M. R., and Boekelheide, K. (2013). Multiple environmental chemical exposures to lead, mercury and polychlorinated biphenyls among childbearing-aged women (NHANES 1999–2004): Body burden and risk factors. *Environ. Res.* **121**, 23–30.

Turci, R., Finozzi, E., Catenacci, G., Marinaccio, A., Balducci, C., and Minoia, C. (2006). Reference values of coplanar and non-coplanar PCBs in serum samples from two Italian population groups. *Toxicol. Lett.* **162**, 250–255.

Viberg, H. (2009). Neonatal ontogeny and neurotoxic effect of decabrominated diphenyl ether (PBDE 209) on levels of synaptophysin and tau. *Int. J. Dev. Neurosci.* **27**, 423–429.

Waller, S. C., He, Y. A., Harlow, G. R., He, Y. Q., Mash, E. A., and Halpert, J. R. (1999). 2,2′,3,3′,6,6′-hexachlorobiphenyl hydroxylation by active site mutants of cytochrome P450 2B1 and 2B11. *Chem. Res. Toxicol.* **12**, 690–699.

Warner, N. A., Martin, J. W., and Wong, C. S. (2009). Chiral polychlorinated biphenyls are biotransformed enantioselectively by mammalian cytochrome P-450 isozymes to form hydroxylated metabolites. *Environ. Sci. Technol.* **43**, 114–121.

Wayman, G. A., Bose, D. D., Yang, D., Lesiak, A., Bruun, D., Impey, S., Ledoux, V., Pessah, I. N., and Lein, P. J. (2012a). PCB-95 modulates the calcium-dependent signaling pathway responsible for activity-dependent dendritic growth. *Environ. Health Perspect.* **120**, 1003–1009.

Wayman, G. A., Impey, S., Marks, D., Saneyoshi, T., Grant, W. F., Derkach, V., and Soderling, T. R. (2006). Activity-dependent dendritic arborization mediated by CaM-kinase I activation and enhanced CREB-dependent transcription of Wnt-2. *Neuron* **50**, 897–909.

Wayman, G. A., Yang, D., Bose, D. D., Lesiak, A., Ledoux, V., Bruun, D., Pessah, I. N., and Lein, P. J. (2012b). PCB-95 promotes dendritic growth via ryanodine receptor-dependent mechanisms. *Environ. Health Perspect.* **120**, 997–1002.

Welshhans, K., and Rehder, V. (2007). Nitric oxide regulates growth cone filopodial dynamics via ryanodine receptor-mediated calcium release. *Eur. J. Neurosci.* **26**, 1537–1547.

Winneke, G. (2011). Developmental aspects of environmental neurotoxicology: Lessons from lead and polychlorinated biphenyls. *J. Neurol. Sci.* **308**, 9–15.

Wu, X., Kania-Korwel, I., Chen, H., Stamou, M., Dammanahalli, K. J., Duffel, M., Lein, P. J., and Lehmler, H. J. (2013). Metabolism of 2,2′,3,3′,6,6′-hexachlorobiphenyl (PCB 136) atropisomers in tissue slices from phenobarbital or dexamethasone-induced rats is sex-dependent. *Xenobiotica* **43**, 933–947.

Wu, X., Pramanik, A., Duffel, M. W., Hrycay, E. G., Bandiera, S. M., Lehmler, H. J., and Kania-Korwel, I. (2011). 2,2′,3,3′,6,6′-Hexachlorobiphenyl (PCB 136) is enantioselectively oxidized to hydroxylated metabolites by rat liver microsomes. *Chem. Res. Toxicol.* **24**, 2249–2257.

Yang, D., Kim, K. H., Phimister, A., Bachstetter, A. D., Ward, T. R., Stackman, R. W., Mervis, R. F., Wisniewski, A. B., Klein, S. L., Kodavanti, P. R., *et al.* (2009). Developmental exposure to polychlorinated biphenyls interferes with experience-dependent dendritic plasticity and ryanodine receptor expression in weanling rats. *Environ. Health Perspect.* **117**, 426–435.